International Journal of Adhesion & Adhesives 44 (2013) 115–121

Contents lists available at SciVerse ScienceDirect

International Journal of Adhesion & Adhesives

journal homepage: www.elsevier.com/locate/ijadhadh

Withdrawal strength of threaded steel rods glued with epoxy in wood

D. Otero Chans *, J. Estévez Cimadevila, E. Martín Gutiérrez

Department of Construction Technology, Universidade da Coruña, Escuela Técnica Superior de Arquitectura, Edificio de Departamentos, Campus de A Zapateira, 15071A Coruña, Spain

ARTICLE INFO

Article history:
Accepted 7 February 2013
Available online 20 February 2013

Keywords:
Epoxy
Wood
Destructive testing
Joint design
Strength

ABSTRACT

In this study, the axial strength of joints made with threaded steel rods glued in timber with epoxy is investigated. Although numerous experimental studies have investigated these joints made in glued laminated timber (glulam) from softwood, experimental data concerning tests on a whole range of hardwood species are still lacking. Thus, to evaluate the influence of timber characteristics on the behaviour of the joint, test results from different species are presented and discussed in this paper. The experimental results from samples using softwood as well as high-density hardwood glued laminated timber are compared. Diverse geometries of the joint are studied in both cases. From this experimental analysis, a formula to predict the strength of the glued-in bars is proposed. The prediction of the strength is made from two parameters that are easily quantifiable the density of the timber and the slenderness of the glued joint. This model shows a good accuracy with the test results of joints made on different species both from softwood and hardwood.

1. Introduction

Joints composed of glued rods began to be used during the 1970s. Initially, they were used to prevent failures due to tension perpendicular to the grain in glued laminated timber (glulam) elements, such as gaps, notches or ridgepoles [1]. Currently, glued-in rods are used for the design of joints in new works due to their high load capabilities and their ability to form rigid joints [2–4]. In addition, they offer great aesthetic benefits and are self-protected by the wood element against weather or fire [5,6]. This type of joint is frequently used in the repair and consolidation of old structures that have been infested by xylophagous organisms or have degraded over time [7].

One of the main problems for the generalization of the use of this type of joint is the limitation of the existing design criteria. European codes do not include a regulated solution for the size of these joints [8]. Therefore, using them requires prior testing in order to assess the strength of this particular solution. As an alternative, several authors have proposed experimental models [9,10] derived mainly from the analysis of joints constructed in glued laminated coniferous timber, which may pose a limitation in application to other types of material. Although the existing models are based on the analysis of joints composed of the same type of wood (glulam from spruce or picea), there are discrepancies regarding the general behaviour criteria of the coniferous wood and the strength values predicted by the proposed expressions [11]. In 1997, Eurocode 5 proposed, as an Informative Annex, a design model likewise limited to joints made in coniferous wood glulam.

Deciduous woods nonetheless offer a great potential for the application of this type of joint because they have higher values of strength and density. These properties are useful both in the design of new structures and in the restoration of old ones. In new structures, the elements of deciduous wood can be used as the main element or merely as transition elements [12,13]. In most old elements, deciduous woods have already been used, at least in certain geographic regions. Deciduous wood provides great strength when designing new projects too. Thus, it is necessary to know the behaviour of the glued rods in any type of wood so as not to limit the possible application of such joints.

Our team made an extensive experimental analysis of threaded steel rods glued with epoxy resins in sawn deciduous woods [14,15]. These test results show important differences in behaviour in comparison with the models proposed in the literature. Based on this work, a new expression was proposed for the design of joints with glued rods in deciduous woods [11,16]. The proposed model showed a very good fit with the results obtained for sawn deciduous woods but required the characterization of the wood used in the joint because it was based on the knowledge of the shear strength of the wood. To address this problem, a new experimental plan was undertaken with two objectives:

- To analyse the factors which have a bearing on the behaviour of the joint, considering the effect of different geometries of the joint and types of wood.

* Corresponding author. Tel.: + 34 981 167 000; fax: + 34 981 167 051.
E-mail addresses: marilo@udc.es (D. Otero Chans), javier@udc.es (J. Estévez Cimadevila), emartin@udc.es (E. Martín Gutiérrez).

0143-7496/$ - see front matter © 2013 Elsevier Ltd. All rights reserved.
http://dx.doi.org/10.1016/j.ijadhadh.2013.02.008

- To validate a design model that can be applied to different types of structural wood, thereby avoiding the need to carry out prior tests to characterize the wood's shear strength.

2. Materials and test methods

Fig. 1 shows the configuration of the test pieces of wood. The pieces had a symmetrical configuration with identical joints at both ends to perform pull–pull tests.

The wood sample pieces were made using two different species of glued laminated timber: spruce (*Picea abies*) and eucalyptus (*Eucaliptus globulus*). The characteristic density values were between 414.93 and 734.83 kg/m^3, and the mean values were between 443.86 and 795.07 kg/m^3, respectively. The samples were stored in a conditioning chamber in an atmosphere normalized at 20 °C and a 65% relative humidity until reaching a balanced 12% humidity. The types of wood selected had extreme densities and strength characteristics within the range of those of the structural woods typically used.

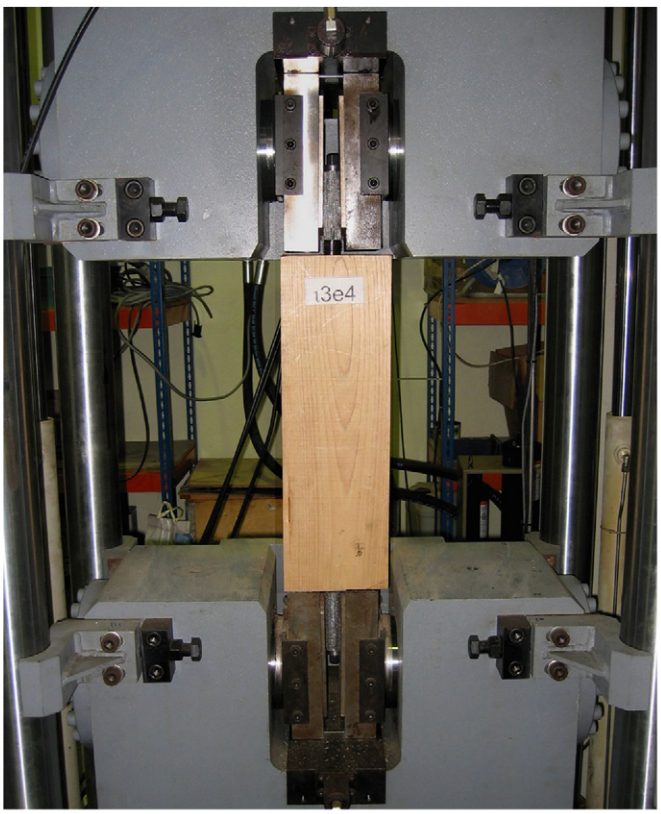

Fig. 1. Testing device.

Threaded rods of high-strength steel, 12.9 grade [17], with diameters of 12 mm were used. This diameter allowed for the design of different types of outer connections, both glued and threaded in auxiliary joint elements [12]. High-strength steel was chosen to prevent failure due to rod yield, which would make it impossible to evaluate the true load capability of the glued joint. In practice, the use of lower quality steel is recommended to achieve ductile failure associated with the tension in the rod [7,18–20]. The threaded bars also guaranteed the mechanical transfer of the load between the steel and the adhesive, allowing the selection of an ideal adhesive formulation for the wood [13, 21].

The geometrical parameters are described in Table 1. The wooden pieces had a cross section of 160 × 160 mm (a), which yielded an upper edge distance (c) greater than six times the diameter of the rod. This distance was much greater than the one recommended in the literature [8, 10, 20], limiting the possibility of premature failures by splitting in the wood. The length of the piece of wood was three times that of the anchorage length of the rods (L). This configuration provided a distance between the internal ends of rods (L_i) equal to the anchorage length (L). In the tests performed previously and in the literature guaranteed that this distance (L_i) was sufficient to prevent an interaction effect between both inner ends of the bars [22, 23].

The adhesive used was an epoxy resin of two components bisphenol epoxy and aliphatic polyamine (Hilti HIT-RE 500). It is a commercial adhesive that has not been specifically formulated for this application but has yielded good results in previous tests [13–15, 24]. In addition to its strength, it has physical qualities that facilitate the injection of the rods and the caulking of the rods and has limited shrinkage, which is integral to guarantee filling the joint after curing.

The surfaces were not prepared in any way before gluing. Previous experiences have shown that the load transfer between the adhesive and the threaded steel bars is chiefly mechanical [13, 21, 25].

Holes were drilled parallel to the grain with a diameter (D) of 14 mm, guaranteeing an adhesive thickness (e) of 1 mm in the glueline. The length of the holes (L) varied between 60 and 180 mm, with 30 mm increments. This configuration yielded a range of joints with five values of slenderness (λ, understood as

Table 1
Geometric characteristics of the wood sample pieces. Dimensions in mm.

Type of wood sample	**a** Cross section of the piece	**d** Diameter of the rod	**e** Thickness of the glueline	**D** Diameter of the hole	**L** Anchorage length	**Li** Distance between rods	**λ** Slenderness L/d
Type 1	160	12	1	14	60	60	5.0
Type 2	160	12	1	14	90	90	7.5
Type 3	160	12	1	14	120	120	10.0
Type 4	160	12	1	14	150	150	12.5
Type 5	160	12	1	14	180	140	15.0

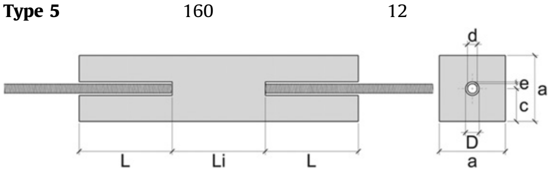

the ratio between the anchorage length and the rod diameter) between 5 and 15. The different types of wood sample pieces tested are listed in Table 1.

The specimens were tested until failure in an INSTRON universal testing machine, equipped with a load cell of 1000 kN. The device had an MTS control system, which was programmed to record the parameters of time, load and displacement during the entire testing process. The load was applied under double tension using a setting device that minimized the effect of possible eccentricities (Fig. 1). The test was conducted with displacement control, adjusting the velocity so that failure occurred in the 5 ± 2 min established for short duration tests.

3. Test results

3.1. Failure modes

The specimens were designed according to conclusions derived from previous studies [13,14], with the objective of exhausting the capacity of the glued joint. Thus, the failure of all of the specimens occurred due to shear rupture on the wood, whether close to the wood-adhesive interface or by the extraction of a block of wood. The failure owing to shear rupture of the wood entails a brittle failure which is highly undesirable in real structures. In practice, it would be advisable to condition the joint's failure to that of yielding of the steel rods in order to ensure the joint's global failure was ductile.

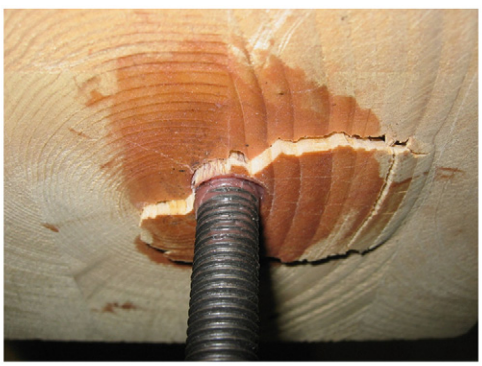

Fig. 2. Failure mode in spruce specimens.

Fig. 3. Failure mode in eucalyptus specimens.

Fig. 2 shows the typical failure mode for specimens made with spruce glulam, and Fig. 3 shows the typical one for specimens made with eucalyptus glulam. The only difference between the failure modes of the two species studied was the place where surface fracture occurred. The extraction of a block of wood adjacent to the glueline was common in the specimens made with the least dense timber (spruce). Specimens made with the denser timber failed at the timber/adhesive interface.

3.2. Failure loads

For each type of wood sample and for each species of wood, eight identical specimens were tested. In some cases, the sample number was reduced to 7, discarding those pieces that had unacceptable drying cracks.

In Table 2, the failure values for each sample are indicated. The characteristic value (F_k) has been determined in accordance with UNE-EN 14358:2007 [26] from the mean value (F_m) and the standard deviation of each one of the samples. The calculation takes the sample size into account. Furthermore, the characteristic value which would correspond to the fifth percentile from the sample ($F_{5\%}$) is considered to be an additional indicative element of the behaviour trend of the results.

Figs. 4 and 5 show the failure loads obtained for each specimen, represented by dots. Unbroken lines represent the mean (F_m) and characteristic (F_k and $F_{5\%}$) loads obtained for each type of wood sample. These values show the trend of the load values in connection with the anchorage lengths of the joints. The results show that the relationship between the failure load and the anchorage length is not linear. The case of 150 mm and 180 mm samples stands out from the rest, as it is shown in Figs. 4 and 5. That is, for short gluing lengths, the failure load increases with anchorage length, but it tends to stabilize, or even decrease, for the longest anchorage lengths.

This behaviour was repeated in the two species tested and ratified the results obtained in previous tests in sawn woods with high densities [13–15]. On the other hand, these results contradicted the traditional design proposals in which the strength of the joint increased linearly with the anchorage length of the rods [8–10,18]; at the same time, these results corroborated other previous approaches which consider non-linear proposals taking the joint's slenderness into account [15, 27]. The existing numerical models also confirm that the relationship between joint's strength (failure load) and its gluing length is not linear [28, 29].

Table 2
Results of the tests (characteristic values for each type).

Type of wood sample	λ	Spruce wood				Eucalyptus wood			
		Failure load [kN] ($F_{5\%}$)	Average shear stress in wood [MPa] ($f_{5\%}$)	Failure load [kN] (F_k)	Average shear stress in wood [MPa] (f_k)	Failure load [kN] ($F_{5\%}$)	Average shear stress in wood [MPa] ($f_{5\%}$)	Failure load [kN] (F_k)	Average shear stress in wood [MPa] (f_k)
Type 1	5.0	23.03	8.73	22.22	8.42	–	–	–	–
Type 2	7.5	26.14	6.60	24.56	6.20	36.64	9.26	33.17	8.38
Type 3	10.0	35.69	6.76	29.01	5.49	44.57	8.44	42.36	8.02
Type 4	12.5	46.33	7.02	40.80	6.18	54.30	8.23	51.55	7.81
Type 5	15.0	44.34	5.60	40.37	5.10	56.77	7.17	54.35	6.86

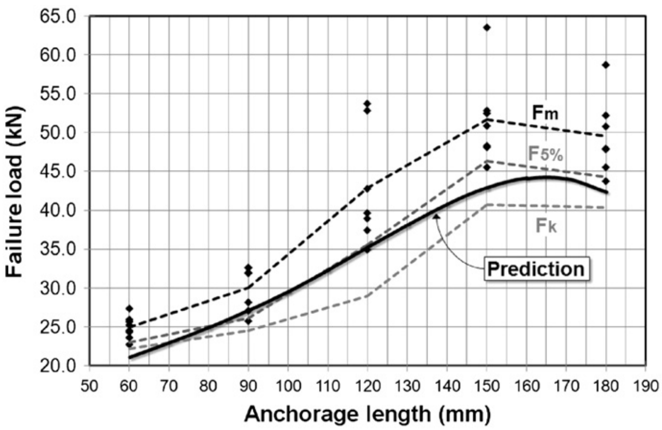

Fig. 4. Failure load values for spruce wood pieces (dots). The broken lines represent the mean and characteristic values. The unbroken line represents the values calculated with the proposed model.

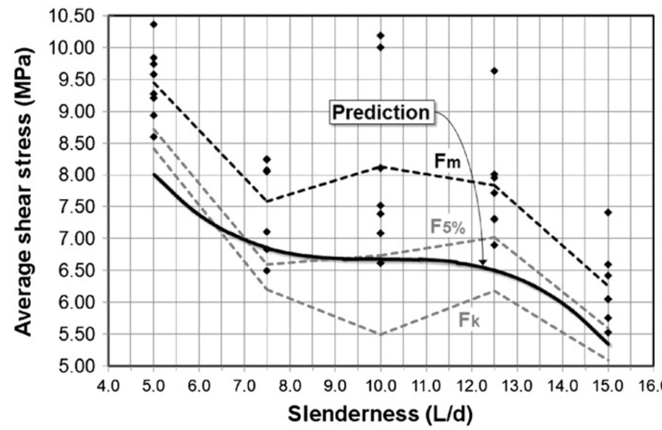

Fig. 6. Average shear failure stress (in MPa) of the joints (spruce wood). The broken lines represent the mean and characteristic values. The unbroken line represents the values calculated with the proposed model.

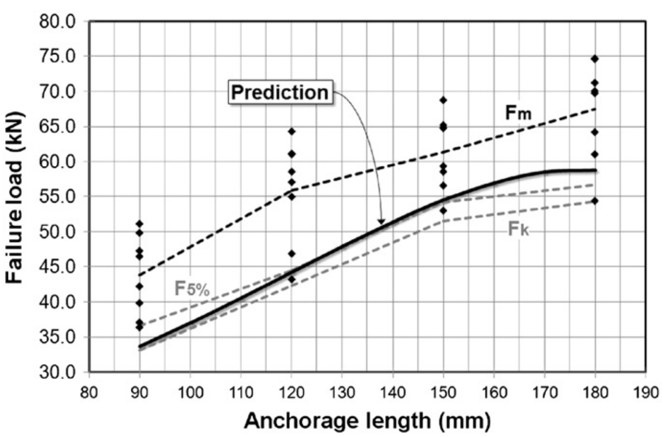

Fig. 5. Failure load values for eucalyptus wood pieces (dots). The broken lines represent the mean and characteristic values. The unbroken line represents the values calculated with the proposed model.

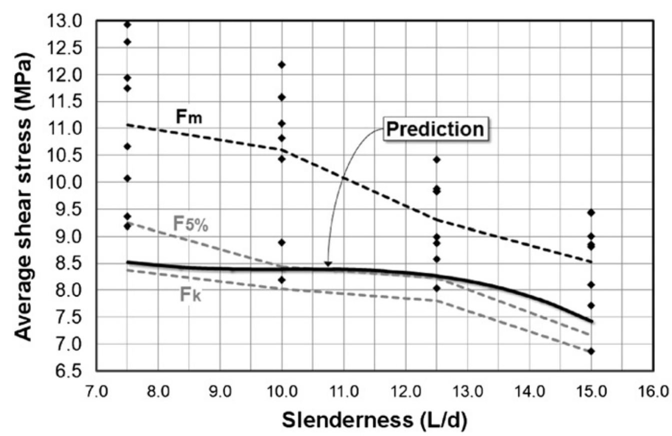

Fig. 7. Average shear failure stress (in MPa) of the joints (eucalyptus wood). The broken lines represent the mean and characteristic values. The unbroken line represents of the values calculated with the proposed model.

Since the failure modes are identical for the different gluing lengths, the explanation to the fact that the strengths drop where the largest lengths are concerned could lie in the so called Volkersen Theory [1, 20]. This theory points to the fact that there are very high stress peaks at the ends of the longest joints, thereby hastening the failure in the joints without taking advantage of the strength in their full length.

4. Discussion

4.1. Influence of the geometry of the joint

Figs. 6 and 7 show the experimental results of the average shear stress on the wood–adhesive contact surface (f, obtained as the ratio between the failure load and the area). The values are represented as a function of the slenderness of the joint (λ). The curves obtained for the mean (f_m) and characteristic (f_k, $f_{5\%}$) values indicate that for lower values of slenderness, failure occurs at higher average shear stress values. These results once more corroborate the conclusions obtained in previous studies conducted on sawn deciduous woods [15] and in coniferous glued laminated timber [19, 30].

From these results, a first criterion of the basic design for this type of joint was extracted, consisting of limiting their slenderness, as the higher average shear stress in failure is reached in joints with lower slenderness. The data obtained recommend not surpassing slenderness values of 15 in the case of low density types of wood, which could reach 18 in the case of more dense types of wood. Fig. 4 shows that above these values, increasing the glued surface does not lead to an increase in the strength of the joint, which would mean a waste of the material.

The comparison between the graphs corresponding to both species shows that the influence of the slenderness is different in both cases. Comparing the mean stresses (f_m) obtained for $\lambda=7.5$ ($L=90$ mm) and $\lambda=15.0$ ($L=180$ mm), we notice that 20% decrease occurs in the case of the spruce and a 25% drop takes place in the case of the eucalyptus.

For medium slenderness values, the average stress value remains or decreases slightly, with variations in the mean stresses (f_m) for slenderness between 7.5 and 15 amounts to 12% for the spruce and to 15% for the eucalyptus. This difference could be due to the fact that the stress distribution along the joint varies significantly with the stiffness of the wood. A FE study [31] showed that timber with higher modulus of elasticity leads to higher stress peaks at the ends of the timber/adhesive interface.

4.2. Influence of the density of the wood

Based on the findings from the previous section, the characteristic density of each type of wood is compared with the average shear stress as a characteristic value ($f_{5\%}$) obtained for each type of wood sample piece. For medium slenderness values

($\lambda=10$), a ratio of 414.93/6.76 was obtained for spruce and 734.83/8.44 for eucalyptus, which indicates that the average shear stress increases with density, although there is no linear proportion between them. An increase of 177% in the density (the difference between spruce and eucalyptus 734.83/414.93) only results in a 125% increase in the average shear strength of the joint (8.44/6.76). This behaviour was repeated for the five slenderness values studied, as may be seen in the values shown in Table 2.

5. Calculations

5.1. Design model to predict the behaviour of the joint

The experimental results shown lead to a design model based on the average shear stresses of the joint (f_{joint}). According to the observations, this parameter can be expressed as a function of the characteristic value of timber density and the geometry of the joint as follows:

$$f_{\text{joint}} = 0.6 \cdot \rho_k^{\alpha} \left(1 - \frac{0.7 \cdot k^3}{\rho_k + k^2} \right) \quad (1)$$

where ρ_k is the characteristic density of the wood (kg/m^3), f_{joint} (N/mm^2), and

$$k = \lambda - 10 = \frac{L}{d} - 10 \quad (2)$$

A suitable fit was obtained with $\alpha=0.4$ for the different species tested. The characteristic load value for the joint (F_k, in Newtons) was obtained from the average stress value in the joint and the wood–adhesive contact surface (Eq. (3)).

$$F_k = f_{joint} \cdot \pi \cdot D \cdot L \quad (3)$$

where f_{joint} is defined in Eq. (1), D (mm) is the diameter of the hole and L (mm) is the anchorage length.

The first part of Eq. (1) ($0.6 \cdot \rho_k^{\alpha}$) represents the shear strength of the joint for average slenderness ($\lambda=10$). The second part corrects the previous value depending on how great the influence of the slenderness is in relation to the wood species used.

Fig. 8 shows the variation of the average shear stress predicted values in the joint as a function of the variation of the slenderness and the density of the wood, according to the proposed model.

One of the great advantages of this design strategy is that the main contributing influence of the mechanical properties of the wood on the strength of the joint is introduced by the density, which is often a known parameter or one that is easy to obtain.

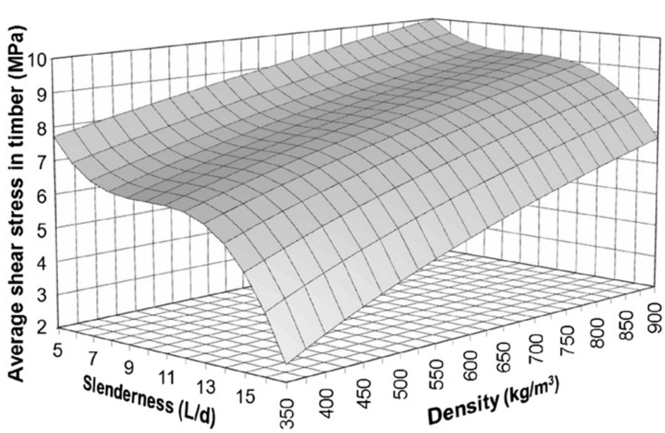

Fig. 8. Graphic representation of the variation in the average shear stress of the joint as a function of the wood density and the slenderness of the joint.

5.2. Comparison of the experimental results with the theoretical prediction

The predicted load values for the different types of joints tested were determined using Eqs. (1)–(3). Figs. 4–7 show the comparison between the experimental values (represented by dots) and the theoretical prediction (represented by a curve). In Figs. 4 and 5 prediction is shown in terms of the load, and in Figs. 6 and 7 it is shown in terms of the average stress in the joint. In addition to this, Table 3 shows the numerical values and the margin of error of the predictions in both cases.

The proposed model was compared with other experimental results obtained previously. These included results based on joints constructed using solid timber of tali *(Erythrophleum ivorense)* and chestnut *(Castanea sativa)* (with characteristic densities of 796.14 and 468.71 kg/m^3, respectively). Threaded steel rods of different diameters glued with epoxy were used with slenderness values between 5 and 18. The methods and devices used have been described in detail in Otero et al. [23, 24]. Fig. 9 shows the graphic representation of the experimental results obtained in the case of chestnut wood and the values predicted using the proposed model (represented by the curved line). A similar fit was obtained with the results corresponding to the tali wood.

5.3. Comparison with other theoretical models

As previously indicated, other approaches have been proposed in past years to account for the behaviour of the joints in relation to their slenderness.

Rossignon et al. [30] proposed an expression which is reflected in the following equation:

$$F_{ax,mean} = 5.8 \cdot \left(\frac{\lambda_h}{10} \right)^{0.44} \cdot \pi \cdot D \cdot L \quad (4)$$

where λ_h is the L/D relationship. The proposal is based on the analysis of joints made in glulam made of Norway spruce lamellas. Threaded steel rods and a two-component epoxy resin were used.

Gehri [19] proposed the so called GSA System, in accordance with the following expression:

$$F_{ax,k} = 40 \cdot A_{shear}^{0.8} \quad (5)$$

where $F_{ax,k}$ (Newton) and A_{shear} (mm^2). The system makes reference to joints made in glulam with a characteristic density of 420 kg/m^3 and rod slenderness lower than 15.

Figs. 10 and 11 show the graphical comparison of the models proposed by Rossignon et al. [30] and Gehri [19] with the one proposed in this paper, in relation to the experimental results obtained for glued laminated timber made from coniferous. Regardless of whether the prediction makes reference to characteristic values in one case (Rossignon) and to average values in another (Gehri-GSA), Figs. 10 and 11 show that the values predicted by these two proposals do not agree with the behaviour pattern seen in the experimental results submitted in this paper.

These models do not take into account the influence of the type of wood, which is why their application is limited to glued laminated coniferous timber. Generally speaking, the literature on this topic does not include any proposals that are applicable to different types of wood. It is, therefore, hard to establish a comparison with other authors with regard to studies on the influence of this particular parameter. Some models, such as the one included by way of an informative annex in the EC5 [8] or the one set forth by Feligioni et al. [32], include the wood density parameter in their design proposals. In both cases, the density is affected by a 1.5-exponent, which has no relationship at all with the experimental results submitted in this paper.

Table 3
Results of the tests (characteristic values for each type) and prediction obtained with the proposed model.

Type of wood sample	Slend. (λ)	Spruce wood					Eucalyptus wood				
		Prediction obtained [kN]	Failure load [kN] ($F_{5\%}$)	Error respect ($F_{5\%}$)	Failure load [kN] (F_k)	Error respect (F_k)	Prediction obtained [kN]	Failure load [kN] ($F_{5\%}$)	Error respect ($F_{5\%}$)	Failure load [kN] (F_k)	Error respect (F_k)
Type 1	5.0	21.16	23.03	−8.1%	22.22	−4, 8%	–	–	–	–	–
Type 2	7.5	27.16	26.14	+3.9%	24.56	+9.5%	33.75	36.64	−7.9%	33.17	+1.7%
Type 3	10.0	35.30	35.69	−1.1%	29.01	+21%	44.35	44.57	−0.5%	42.36	+4.5%
Type 4	12.5	42.98	46.33	−7.2%	40.80	+5.1%	54.62	54.30	0.6%	51.55	+5.6%
Type 5	15.0	42.42	44.34	−4.3%	40.37	+4.8%	58.85	56.77	+3.7%	54.35	+7.6%

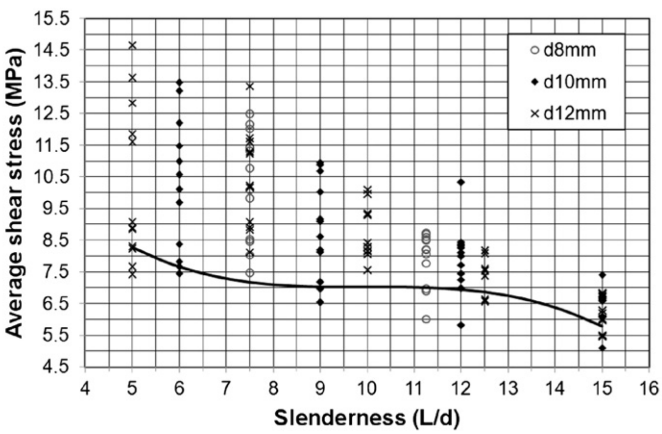

Fig. 9. Representation of the values calculated with the proposed model (line) and experimental values obtained for sawn chestnut timber with different diameters.

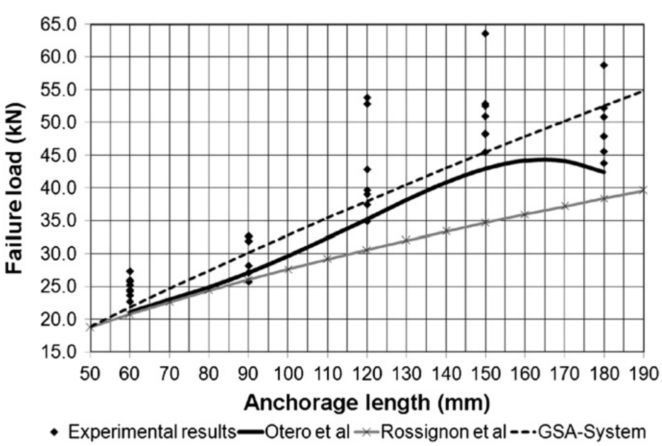

Fig. 10. Load values. Comparison of the predictions made with the proposed model and the models of Rossignon et al. and the GSA-system for laminated spruce wood.

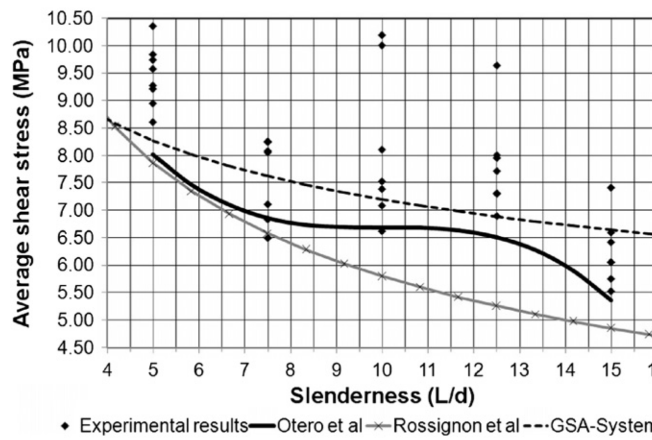

Fig. 11. Average shear stress in the joint. Comparison of the predictions made with the proposed model and the models of Rossignon et al. and the GSA-system for laminated spruce wood.

As has been indicated, the model proposed in Eq. (1) is based on the average shear stress seen in the four wood species studied until now: glulam from spruce and eucalyptus, and solid timber from chestnut and tali. This study has been completed with the influence of slenderness, which ranges from 5 to 18. The proposed model agrees with the common behaviour pattern noticed and predicts the joint's strength with error ranges which are generally below 10%.

6. Conclusions

The experimental study of joints made with threaded steel rods glued with epoxy in different types and species of wood showed that the strength of the joint is conditioned by its geometry and by the strength characteristics of the species of wood used.

The comparative analysis of our test results showed a behaviour pattern that is independent from the type of wood that is used, qualitatively speaking. In this pattern, the strength of the joint increases with the density of the wood being used, and the density is likewise related to the strength characteristics of the type of wood in question. The relationship between the increase in the load capacity of the joint and the timber density does not show a linear trend.

For the geometric characteristics of the joint, the average shear stress at which there is joint failure is drastically reduced for large anchorage lengths; in other words, joints with longer gluing length do not lead to higher joint strength.

The joints constructed with more dense types of wood are less affected by the slenderness of the joint.

Finally, the comparison between our experimental results and those obtained with the design model proposed here showed a good agreement for different types of wood (sawn and glued laminated timber) and for different species (coniferous and deciduous ones), with a high range of densities. The prediction of the axial strength of the joint can be obtained, for the tested combinations of material and geometry parameters, from two parameters that are easily quantifiable: the slenderness of the joint and the density of the wood used. More experimental work needs to be done to assess the predictions' accuracy for different combinations of material and geometrical parameters.

Acknowledgements

This research was sponsored by the Ministry of Innovation and Industry (Xunta de Galicia) through a research project entitled

"Sistemas de mejora de la tecnología de la unión con adhesivos de barras de acero insertadas en madera" (Systems to improve the technology of joints made with steel rods glued in timber). The financial support is gratefully acknowledged.

References

[1] Johansson C-J. Glued-in bolts, Step1: lecture C14. In: βlass HJ, editor. Netherlands: Almere; 1995.
[2] Aicher S, Herr J. Investigations on high strength glulam frame corners with glued-in steel connectors, 5th World conference on timber engineering, Montreux, Switzerland, 1998.
[3] Guan ZW. Structural behaviour of glued joints using FRP, 5th World conference on timber engineering, Montreux, Switzerland, 1999.
[4] Kuhlmann U, Aicher S, Lippert P. Rigid frame corners with glued-in rods, Joints in timber structures, . In: Proceedings of the international RILEM symposium, Stuttgart, Germany, 12–14 September 2001.
[5] Buchanan AH, Barber DJ. Fire resistance of epoxied steel rods in glulam. In: Proceedings, 1994 pacific timber engineering conference, Gold Coast, Australia, 1994, vol. 1, p. 590–98.
[6] Park J-S, Buchanan AH, Lee J-J. Fire performance of laminated Veneer lumber with glued-in steel rods connections. J.. Fire Sci 2006;24(1):27–46.
[7] Broughton JG, Hutchinson AR. Review of relevant materials and their requirements for timber repair and restoration, LICONS (low intrusion conservation systems for timber structures, CRAF-1999-71216, Task 2.2, 2003.
[8] Eurocode 5 prEN 1995-2 Second draft, Draft rules for bonded-in rods. Design of timber structures. Extract from: design of timber structures. Part 2: Bridges. CEN/TC 250/SC5, 2003.
[9] Kangas J. Joints of glulam structures based on glued ribbed steel rods, VTT Publications, 196 (1994), Technical research centre of Finland, Espoo.
[10] Riberholt H. Glued bolts in Glulam, Department of structural engineering, Series R, No. 210, Technical University of Denmark, 1986.
[11] Otero Chans D. Barras roscadas de acero encoladas en madera de frondosa, (English title: Threaded steel rods glued in hardwood timber), PhD thesis, Universidade da Coruña 2007.
[12] Estévez Cimadevila J, Vázquez Rodríguez JA. Spatial truss o hollow bars made of laminated timber supported by walls of reinforced masonry. J Int Assoc Shell Spatial Struct 2004;45(1):13–21.
[13] Otero Chans D, Estévez Cimadevila J, Martín Gutiérrez E. Glued joints in hardwood timber. Int J Adhes Adhes 2008;28:457–63.
[14] Estévez Cimadevila J, Vázquez Rodríguez JA, Otero Chans D. Experimental behaviour of threaded steel rods glued into high-density hardwood. Int J Adhes Adhes 2007;27:136–44.
[15] Otero Chans D, Estévez Cimadevila J, Martín Gutiérrez E. Model for predicting the axial strength of joints made with glued-in rods in sawn timber. Constr Build Mater 2010;24:1773–8.
[16] Otero Chans D, Estévez Cimadevila J, Martín Gutiérrez E. Análisis experimental de uniones con barras de acero encoladas en maderas de castaño y elondo. Materiales de Construcción 2010;60:111–25.
[17] UNE-EN 1993-1-1, Eurocode 3: Design of steel structures – Part 1-1: General rules and rules for buildings, CEN/TC 250, 2008.
[18] Buchanan A, Moss P. Design of epoxied steel rods in glulam timber, PTEC'99. Pacific timber engineering Conference, Proceedings vol. 3, In: Walford GB, Gaunt DJ, editors. Forest Research Bulletin No. 212, 1999, p. 286–293.
[19] Gehri E. High performing jointing technique using glued-in rods, 11th World Conference on Timber Engineering WCTE, Riva del Garda, Italy. 20–24 June, 2010.
[20] Tlustochowicz G, Serrano E, Steiger R. State-of-the-art review on timber connections with glued-in steel rods. Mater Struct 2011;44(59):997–1020.
[21] Bernasconi A. Axially loaded glued-in rods for high capacity joints – Behaviour and resistance, PRO22: joints in timber structures. In: Proceedings of the International RILEM Symposium, Stuttgart, Germany, 12–14 September 2001.
[22] Aicher S, Höfflin L, Wolf M. Influence of specimen geometry on stress distributions in pull-out tests of glued-in steel rods in wood. Otto-Graf-J 1998;9:205–17.
[23] Otero Chans D, Estévez Cimadevila J, Martín Gutiérrez E. Strength of joints with epoxy-glued threaded steel rods in tali Timber. J Mater Civil Eng ASCE 2011;23:453–8.
[24] Otero Chans D, Estévez Cimadevila J, Martín Gutiérrez E. Influence of the geometric and material characteristics on the strength of glued joints made in chestnut timber. Mater Des 2009;30:1325–32.
[25] Bengtsson C, Kemmsies M, Johansson C-J. Production control methods for glued-in rods for timber structures, World Conference on Timber Engineering, Whistler Resort, British Columbia, Canada, July 31–August 3, 2000.
[26] UNE-EN 14358, Timber structures – calculation of characteristic 5-percentile values and acceptance criteria for a sample, AEN/CTN 56, 2007.
[27] Gerold M. Verbund van Holz und Gewindestangen aus Stahl. Bautechnik 1992;69(4):167–78.
[28] Gustafsson P-J, Serrano E, Aicher S, Johansson C-J. A strength design equation for glued-in rods, PRO22: joints in timber structures, In: Proceedings of the International RILEM symposium, Stuttgart, Germany, 12–14 September 2001.
[29] Serrano E. Glued-in rods for timber structures- A 3D model and finite element parameter studies. Int J Adhes Adhes 2001;21(2):115–27.
[30] Rossignon A, Espion B. Experimental assessment of the pull-out strength of single rods bonded in glulam parallel to the grain. Holz Roh Werkst 2008;66:419–32.
[31] Martín Gutiérrez E, Estévez Cimadevila J, Otero Chans D, Vázquez Rodríguez JA. Análisis numérico del comportamiento de soluciones de anclaje en madera mediante barras roscadas encoladas, 1th Congreso Ibero-LatinoAmericano de la Madera en la Construcción, CIMAD 2011, Coimbra, 2011.
[32] Feligioni L, Lavisci P, Duchanois G, de Ciechi M, Spinelli P. Influence of glue rheology and joint thickness on the strength of bonded-in rods. Holz Roh Werkst 2003;61(4):281–7.